Diffusible Crosslinkers Generate Directed Forces in Microtubule Networks

Graphical Abstract

Non-enzymatic **crosslinkers** diffuse in **microtubule** overlaps, **with the overlap ends confining the diffusion**.

Entropic expansion of the diffusible crosslinkers **generates a force**, which causes unidirectional microtubule sliding.

Entropic forces are determined by optical tweezers and theory to be **in the pN range**.

Time
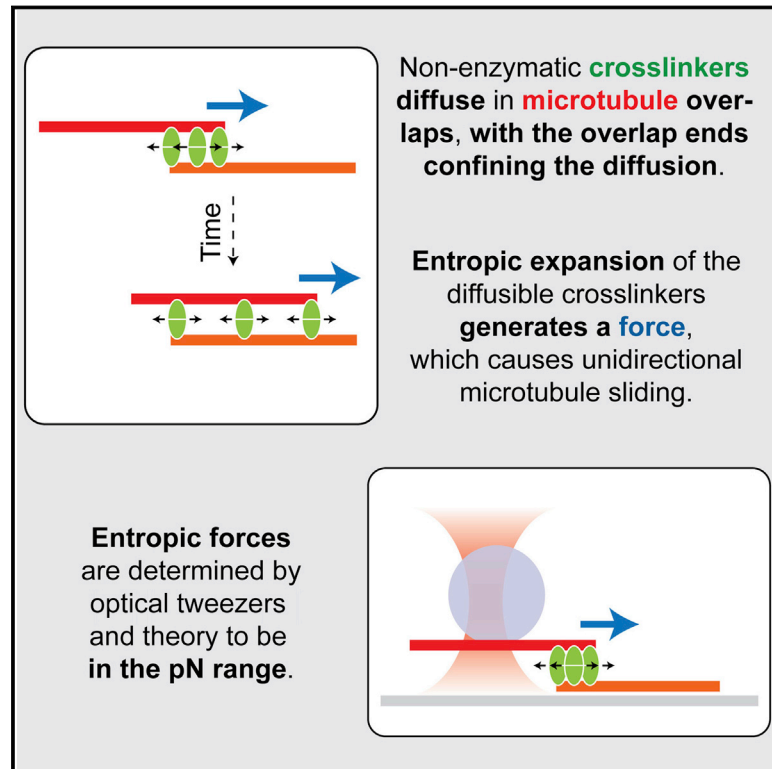
Authors

Zdenek Lansky, Marcus Braun, ...,
Marcel E. Janson, Stefan Diez

Correspondence

tenwolde@amolf.nl (P.R.t.W.),
marcel.janson@wur.nl (M.E.J.),
diez@bcube-dresden.de (S.D.)

In Brief

Mechanical force on the same scale as force induced by microtubule-crosslinking motor proteins can be generated in microtubule networks by passive diffusion of crosslinkers in confined spaces between cytoskeletal filaments

Highlights

- Diffusible crosslinkers confined in microtubule overlaps can generate directed forces

- Thermal motion of the crosslinkers is harnessed to perform mechanical work

- Force generation is quantitatively explained by entropic expansion of crosslinkers

CellPress

Diffusible Crosslinkers Generate Directed Forces in Microtubule Networks

Zdenek Lansky,[1,2,5] Marcus Braun,[1,2,5] Annemarie Lüdecke,[1] Michael Schlierf,[1] Pieter Rein ten Wolde,[3,*] Marcel E. Janson,[4,*] and Stefan Diez[1,2,*]

[1]B CUBE - Center for Molecular Bioengineering, Technische Universität Dresden, Arnoldstrasse 18, 01307 Dresden, Germany
[2]Max Planck Institute of Molecular Cell Biology and Genetics, Pfotenhauerstrasse 108, 01307 Dresden, Germany
[3]AMOLF, Science Park 104, 1098 XG Amsterdam, the Netherlands
[4]Laboratory of Cell Biology, Wageningen University, Droevendaalsesteeg 1, 6708 PB Wageningen, the Netherlands
[5]Co-first author
*Correspondence: tenwolde@amolf.nl (P.R.t.W.), marcel.janson@wur.nl (M.E.J.), diez@bcube-dresden.de (S.D.)
http://dx.doi.org/10.1016/j.cell.2015.01.051

SUMMARY

Cytoskeletal remodeling is essential to eukaryotic cell division and morphogenesis. The mechanical forces driving the restructuring are attributed to the action of molecular motors and the dynamics of cytoskeletal filaments, which both consume chemical energy. By contrast, non-enzymatic filament crosslinkers are regarded as mere friction-generating entities. Here, we experimentally demonstrate that diffusible microtubule crosslinkers of the Ase1/PRC1/Map65 family generate directed microtubule sliding when confined between partially overlapping microtubules. The Ase1-generated forces, directly measured by optical tweezers to be in the piconewton-range, were sufficient to antagonize motor-protein driven microtubule sliding. Force generation is quantitatively explained by the entropic expansion of confined Ase1 molecules diffusing within the microtubule overlaps. The thermal motion of crosslinkers is thus harnessed to generate mechanical work analogous to compressed gas propelling a piston in a cylinder. As confinement of diffusible proteins is ubiquitous in cells, the associated entropic forces are likely of importance for cellular mechanics beyond cytoskeletal networks.

INTRODUCTION

Diffusion, originating from the random, thermal motion of molecules, is one of nature's most important transport mechanisms. It can be exploited for the generation of directed forces when the molecules are spatially confined. An every-day example is a gas spring, where the expansion of a gas compressed in a cylinder can be understood as an entropy-driven process that maximizes the total number of microscopic states the system can adopt. We here ask if, analogously, subcellular mechano-systems like cytoskeletal networks, can harness the entropic forces arising from the confinement of diffusible molecules.

In many cellular systems, the molecules are not confined to three dimensions, but rather to two dimensions or even to one dimension. A prominent example of the latter is the diffusion of proteins along microtubules (Helenius et al., 2006). Moreover, the ends of microtubules have been shown to constitute diffusion barriers for proteins involved in forcefully tethering kinetochores to the shrinking ends of depolymerizing microtubules (Asbury et al., 2006; Gestaut et al., 2008; Powers et al., 2009), as well as for diffusible microtubule crosslinkers (Braun et al., 2011). An example of a diffusible microtubule crosslinker is *S. pombe* Ase1 (a member of the Ase1/PRC1/Map65 family), which is believed to stabilize bipolar microtubule arrays. Ase1 localizes to the anti-parallel microtubule overlaps in the midzone of the mitotic spindle during anaphase (Yamashita et al., 2005) and to the anti-parallel microtubule overlaps of the interphase microtubule array (Loïodice et al., 2005). While forces generated by molecular motors and dynamic microtubules are believed to be the main contributors to the remodeling of both of these bipolar microtubule structures (Civelekoglu-Scholey and Scholey, 2010; Janson et al., 2007; Peterman and Scholey, 2009), bipolar microtubule arrays are destabilized and break down in the absence of Ase1 (Loïodice et al., 2005; Schuyler et al., 2003; Yamashita et al., 2005). Since Ase1 crosslinkers slow down microtubule-microtubule sliding (Braun et al., 2011; Janson et al., 2007), friction forces by microtubule-bound Ase1 may thus be required to balance motor forces within networks. Still, because Ase1 can diffuse in the confined space of microtubule overlaps (Braun et al., 2011; Kapitein et al., 2008), we reasoned that Ase1, apart from generating friction, might also generate entropic forces.

We here devised a well-controlled experimental assay to confine small numbers of Ase1 diffusible crosslinkers in between two partially overlapping microtubules. Using total-internal reflection fluorescence (TIRF) microscopy, we showed that the entropic expansion of the confined crosslinkers is strong enough to induce the directed sliding of the microtubules with respect to each other. We directly measured the entropic forces generated by Ase1 in the expanding overlaps using optical tweezers and found them to be in the piconewton (pN) range. This suggests that the entropy of the crosslinkers in an overlap can generate biologically relevant forces that are on the same scale as forces induced by microtubule-crosslinking motor proteins. To test this hypothesis, we employed kinesin-14 motor proteins and found
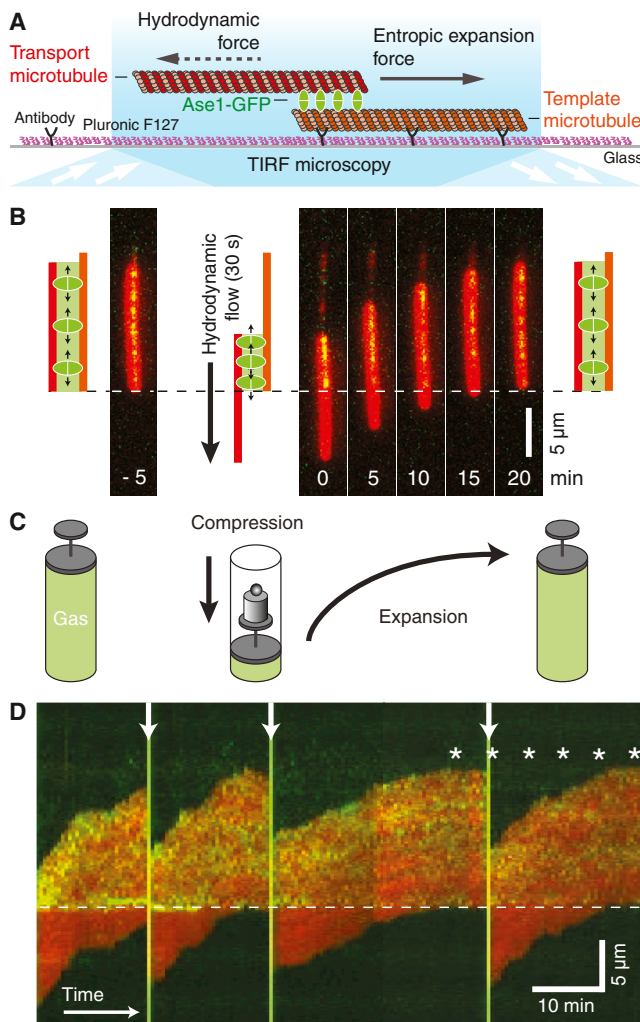
Figure 1. Entropic Expansion of Diffusible Ase1-GFP Crosslinkers Induces the Directed Sliding of Partially Overlapping Microtubules

(A) Schematic representation of Ase1-driven sliding of a transport microtubule (red) along a surface-immobilized template microtubule (orange).

(B) Typical time-lapse fluorescence, multichannel micrographs showing the positions of a transport microtubule (red channel) as a function of time before and after flow-induced compression of Ase1-GFP (green channel) within a microtubule overlap. Prior to imaging, free Ase1-GFP was removed from solution. Schematic diagrams illustrate the positions of the microtubules before and immediately after the application of the hydrodynamic flow, as well as at the end of the experiment. The end of the template microtubule is indicated by the dashed line.

(C) A gas spring, the macroscopic analog of the molecular Ase1-microtubule system, expands when the external load is decreased.

(D) Extended kymograph showing multiple cycles of the experiment described in (B). Time points and direction of flow application are indicated by the vertical arrows. Asterisks indicate the time of the snapshots presented in (B). The end of the template microtubule is indicated by the dashed line. Regions with enhanced localization of Ase1-GFP signal correspond to the microtubule overlap. See also Movie S1.

that motor-driven microtubule-microtubule sliding could indeed be reversed by the addition of Ase1. We quantitatively describe the force generation by Ase1 by a statistical-mechanical model,

which predicts the expansion force to follow the ideal gas law. Taken together, our results show that Ase1 diffusible cross-linkers confined between partially overlapping microtubules create a pressure, analogously to gas molecules confined in a cylinder by a piston. Our results are a demonstration of the unexpected effects entropy may have in cells. We suggest that forces generated by diffusible crosslinkers of the Ase1/PRC1/MAP65 family are likely of importance in the midzone of the mitotic spindle, where they may regulate the motorized sliding of anti-parallel microtubules.

RESULTS

Entropic Expansion of Diffusible Ase1-GFP Crosslinkers Induces the Directed Sliding of Partially Overlapping Microtubules

To study force generation by confined Ase1 crosslinkers in vitro, we generated overlapping microtubules by (1) immobilizing dimly rhodamine-labeled "template" microtubules on a coverslip, (2) allowing 50 picomolar (pM) Ase1-GFP to bind diffusively to the immobilized template microtubules, and (3) flushing in brightly rhodamine-labeled "transport" microtubules to bind to the template microtubules using a solution without Ase1-GFP; this effectively removed Ase1-GFP molecules that were not bound to the template microtubules (Figure 1; Experimental Procedures). We then applied hydrodynamic flow of assay buffer without Ase1-GFP to slide the transport microtubules along the template microtubules, generating partial overlaps with reduced overlap lengths (Figures 1A and 1B). Due to their high affinity for microtubule overlaps, as compared to their lower affinity for single microtubules (Braun et al., 2011), the diffusible Ase1-GFP molecules did not leave the overlap regions during this process. The reduction in the overlap lengths consequently led to an increased confinement of the crosslinkers. As soon as the flow stopped, the overlap lengths increased through directed sliding of the transport microtubules (Figure 1B and Movie S1). During this expansion, the confined Ase1-GFP molecules redistributed themselves uniformly within the overlap regions by one-dimensional diffusion. Again, no Ase1-GFP molecules were lost as evidenced by the constancy of the integrated Ase1-GFP fluorescence intensity along the overlap regions (Figure S1B). Compression and expansion could be cyclically repeated (Figure 1D and Movie S1), resembling the macroscopic mechanism of a gas spring (Figure 1C).

Quantification of the Forces Generated by Ase1-GFP Confined between Partially Overlapping Microtubules Using Optical Tweezers

We quantified the forces generated by Ase1 confined between partially overlapping microtubules by optical tweezers (Figure 2). First, we formed microtubule overlaps in a similar manner as in the previous experiment (Experimental Procedures). In the absence of Ase1-GFP in solution, we attached a silica microsphere to a transport microtubule by optical tweezers. Using a piezo translation stage, we then moved the template microtubule in steps relative to the laser trap in the direction along the longitudinal axis of the template microtubule, forming partial microtubule-overlaps and compacting Ase1-GFP until the two microtubules were pulled apart (Figures 2A, 2B, S2A, and S2B
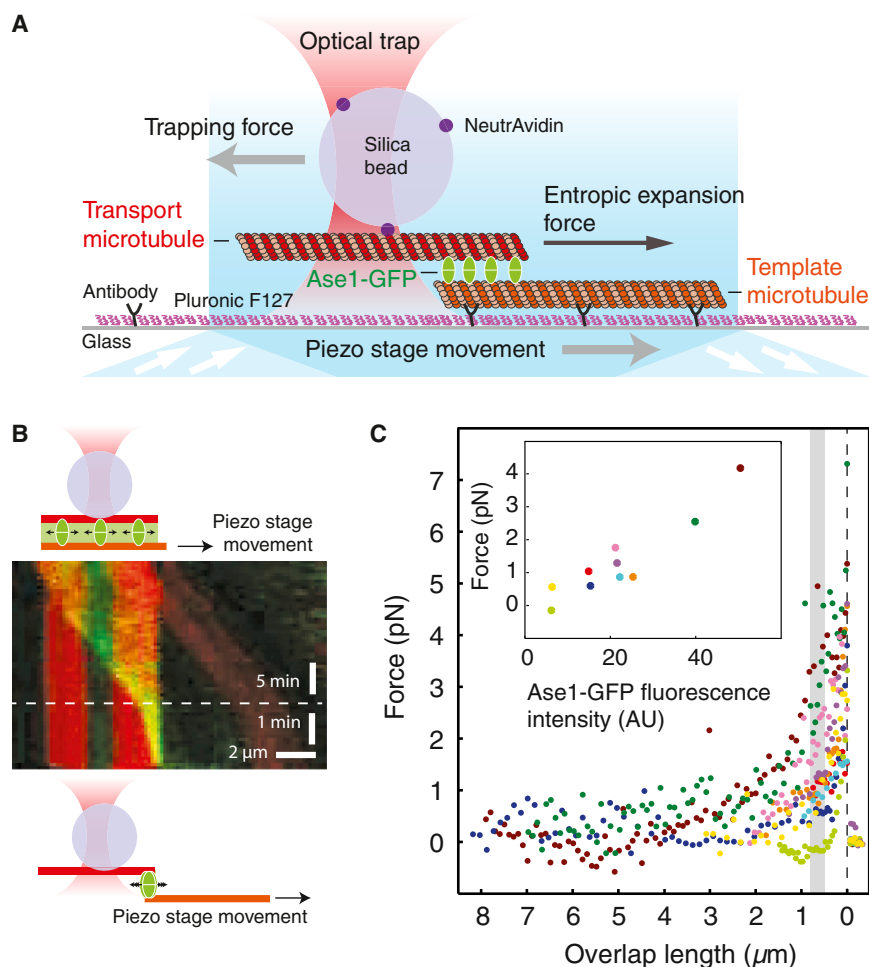
A

Optical trap

Trapping force

Silica bead

NeutrAvidin

Transport microtubule

Entropic expansion force

Ase1-GFP

Template microtubule

Antibody   Pluronic F127

Glass

Piezo stage movement

B

Piezo stage movement

5 min
1 min
2 µm

Piezo stage movement

C

Force (pN)

Ase1-GFP fluorescence intensity (AU)

Overlap length (µm)

Figure 2. Quantification of the Entropic Forces Generated by Ase1-GFP Confined between Partially Overlapping Microtubules by Optical Tweezers

(A) Schematic representation of the optical tweezers experiment. A trapped, NeutrAvidin-coated silica bead (not drawn to scale) is attached to a biotinylated transport microtubule (red). In order to slide the microtubules relative to each other, the template microtubule (orange) was moved by a piezo translational stage, while keeping the center of the laser trap at a fixed position.

(B) Typical multichannel kymograph showing the movement of the dimly labeled template microtubule (driven by the movement of the piezo stage) relative to the trapped, brightly labeled transport microtubule in the absence of free Ase1-GFP in solution. The density of Ase1-GFP increased in the shortening overlap. Approximately 2 min before the separation of the microtubules, the movement of the piezo stage was slowed down to obtain a higher number of data points. The bleached spot in the middle of the transport microtubule is caused by the focused trapping laser. The region with enhanced localization of Ase1-GFP signal corresponds to the microtubule overlap. For snapshots of the event see Figure S2A. See also Movie S2.

(C) Equilibrium bead displacements, corresponding to the steady-state forces induced by the confined Ase1-GFP in the overlaps, as function of overlap length. Presented are ten independent measurements. The inset shows the measured forces as function of Ase1-GFP fluorescence intensity in the overlap averaged for overlaps with lengths between 0.6 and 0.8 µm (denoted by the gray box in the main panel; same color-coding of measurements). Overlap lengths and forces were offset-corrected by assuming that the overlap length is zero right before the microtubules were pulled apart (dashed line) and that the force is zero after the microtubules were pulled apart.

and Movie S2). After each step, we allowed the system to equilibrate before measuring the force. We found that the force increased with decreasing overlap length, reaching values up to 3.7 ± 1.8 pN (average ± SD, n = 10) just before the two microtubules were pulled apart (Figure 2C). The observed forces increased linearly with increasing Ase1-GFP densities in the overlaps as inferred from fluorescence intensities (Figures 2C, inset, and S2C; Experimental Procedures).

Modeling the Ase1-Induced Expansion of Partial Microtubule-Overlaps

To explain the origin of the observed forces generated by Ase1, we analytically modeled the mutually exclusive binding of crosslinkers to discrete binding sites along a single protofilament in a microtubule overlap (Figure 3). For the case of a constant number of confined crosslinkers in the overlap; i.e., when no crosslinkers bind into or unbind from the overlap (scenario as in Figures 1 and 2), the entropic expansion force, F, acting on the transport microtubule is found to be given by the one-dimensional analog of the ideal gas law $FL \cong nk_BT$ (Extended Results, Text 1). Here, L is the overlap length and n is the number of

crosslinkers within the overlap, k_B is the Boltzmann constant, and T is the absolute temperature. This model predicts that the force increases linearly with the density of the crosslinkers in the overlap, as observed in our experiments (Figures 2C, inset, and S2C). While a quantitative test of the predicted relation between force and crosslinker density is not possible due to experimental uncertainties in overlap lengths and protein numbers, the range of maximum measured forces is predicted correctly. The model predicts the generation of forces in the 1 pN range when the crosslinkers are maximally compressed between two microtubule protofilaments, that is when all binding sites within the overlap are fully occupied by Ase1. Structural work on Ase1 homologs suggests that such high densities of crosslinkers are indeed possible (Subramanian et al., 2010). The observed maximal forces of 3.7 ± 1.8 pN may indicate that multiple rows of Ase1 crosslinkers bind to neighboring protofilaments in the overlap (Extended Results, Text 1).

We next investigated whether entropic forces, in combination with frictional drag exerted by the Ase1 crosslinkers, can also explain the observed sliding velocities of transport microtubules
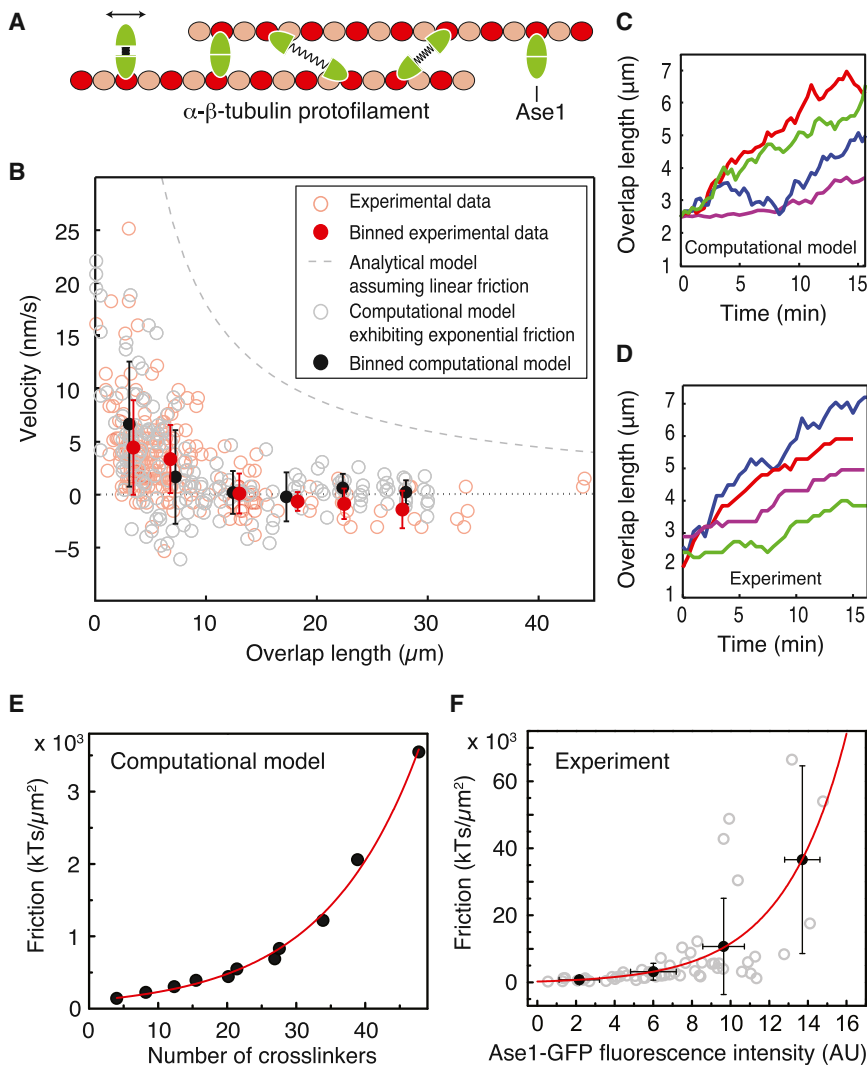
Figure 3. Ase1-GFP Entropy Together with an Exponential Scaling of Friction Explain the Expansion of Microtubule Overlaps in the Absence of Ase1-GFP in Solution

(A) Schematic representation of the modeled geometry. Microtubules are modeled as a one-dimensional array of lattice sites. For the computational model, microtubule-Ase1-microtubule links are simulated as harmonic springs, whose ends can hop individually between neighboring lattice sites. The spring constant is chosen to match the measured diffusion rates of Ase1-GFP on single microtubules and in microtubule overlaps. Rate constants for crosslinker binding and unbinding are in agreement with the measured dissociation constants (Figures S3A and S3B; Extended Results, Texts 1–4; Table S1).

(B) Averaged velocities of Ase1-GFP induced microtubule sliding as function of overlap length. Shown are experimental data (red open circles, 95 events, 48 microtubules in experiments as presented in Figure 1B), results from the analytical model (gray dashed line, $v_{MT} = 2\,D_{Ase1}^{MT}/L$ with $D_{Ase1}^{MT} = 0.085 \pm 0.007\ \mu m^2\ s^{-1}$ assuming a constant number of Ase1-GFP in the overlap), as well as results from the computational model (gray open circles, total of 24 simulation runs, parameters summarized in Table S1). In the computational model, the initial number of crosslinkers n_0 and initial overlap lengths L_0 were chosen from the experimentally observed range of $n_0 = 10, 20, 50$, and L_0 randomly between 0.1 and 30 μm, respectively. The overlaps were allowed to expand for at least 15 min. Solid red and black circles represent the binned averages ($\pm$SD) of the experimental data and the computational model, respectively. Data points (overlap lengths ranging from 0 to 30 μm) were binned in six equidistant bins with a width of 5 μm.

(C and D) Typical time traces of overlap expansions obtained from the computational model (C, data as shown in Movie S3 and summarized in Figure 3B) and from the experiments (D, data as shown in Figure 1B and Movie S1 and summarized in Figure 3B). Different colors represent individual events. The variability in the time traces reflects the stochasticity of the underlying force-generating mechanism.

(E) Results of the computational model predicting that friction increases exponentially with the number of crosslinkers. The diffusion constants of transport microtubules on an infinitely long template microtubule were determined by computing their mean-square displacements as a function of time, for different numbers of crosslinkers. Friction coefficients γ were calculated from the computed diffusion coefficients D using $\gamma = k_B T/D$. The simulation parameters are summarized in Table S1.

(F) Experimental results showing that friction increases exponentially with the number of Ase1-GFP crosslinkers, as inferred from the Ase1-GFP fluorescence intensity integrated along the overlap region. Friction coefficients were calculated from the diffusion of single transport microtubules (Figure S3D and Movie S4) by the same procedure as in (C). Friction coefficients (n = 56 diffusing microtubules) were binned according to the Ase1-GFP fluorescence intensity measured in the overlap during the movement into four equidistant bins with the width of 4 AU (solid black circles represent averages $\pm$SD).

in absence of external load (scenario as in Figure 1). The viscous drag exerted by the solution was neglected due to its small contribution at low velocities (Hunt et al., 1994; Tawada and Sekimoto, 1991). We described the frictional drag coefficient γ of a single Ase1-microtubule link following the Einstein relation $\gamma = k_B T/D_{Ase1}^{MT}$ (Einstein, 1906), where D_{Ase1}^{MT} is the diffusion constant of a single Ase1 molecule on a single microtubule. Assuming a linear dependence of the frictional drag on the number of diffusible crosslinkers (Tawada and Sekimoto, 1991), the velocity of overlap expansion is given by $v_{MT} = 2\,D_{Ase1}^{MT}/L$

(Extended Results, Text 2). This analytical expression, independent of the number of crosslinkers in the overlap, qualitatively reproduced the trend of the measured velocities (Figure 3B). However, it overestimated the absolute values, suggesting that friction might be underestimated in our analytical model.

Friction between Crosslinked Microtubules Depends Exponentially on the Number of Crosslinkers

To explain the magnitude of entropy-driven sliding velocities quantitatively, we set up a particle-based, computational model
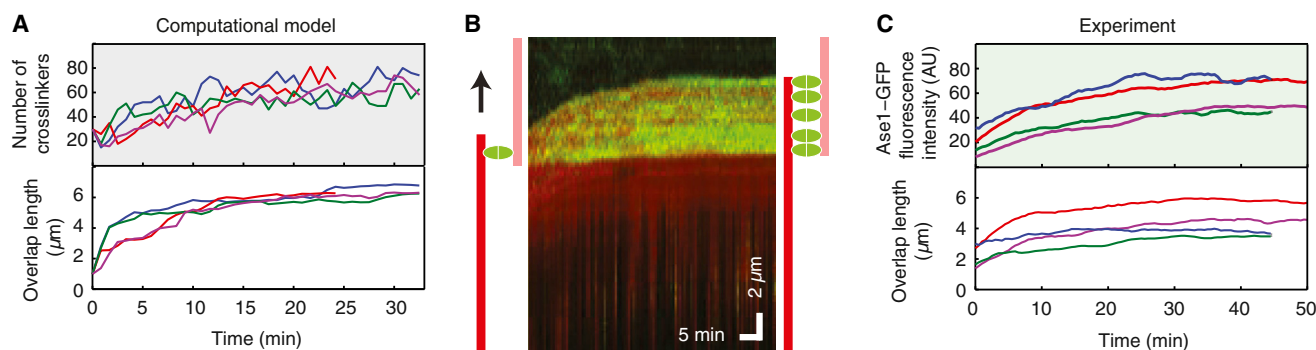
Figure 4. Overlap Expansion Slows Down in the Presence of Ase1-GFP in Solution

(A) Typical simulated time traces (computational model) of overlap length and number of crosslinkers in the overlap during microtubule sliding in the presence of Ase1 in solution. At 0.1 nM Ase1 concentration, overlap expansion comes to an apparent stall before reaching full overlap (20 μm in this particular case). Model parameters are listed in Table S1; the initial number of crosslinkers was 30. Different colors represent individual simulated events. The variability in the time traces reflects the stochasticity of the underlying mechanism.

(B) Typical multichannel kymograph of Ase1-GFP driven sliding of a transport microtubule (red) in the presence of 17 pM Ase1-GFP (green) in solution. In contrast to experiments with a constant number of Ase1-GFP in the overlap (see Figures 1 and 3), sliding comes to a halt due to the increase in the number of Ase1-GFP molecules, and thus the Ase1-GFP induced friction, in the expanding overlap. The region with enhanced localization of Ase1-GFP signal corresponds to the microtubule overlap.

(C) Typical experimental time traces (out of 15 captured events) of overlap length and number of crosslinkers (data as presented in the kymograph in Figure 4B). Different colors represent individual events. The variability in the time traces reflects the stochasticity of the underlying mechanism.

in which the microtubule-Ase1-microtubule links are described as harmonic springs whose ends can hop between neighboring binding sites within an overlap formed by two opposing protofilaments (Figure 3A; Extended Results, Text 3). The spring constant of the individual microtubule-Ase1-microtubule links was estimated from the about 8-fold lower diffusion coefficient of Ase1-GFP in microtubule overlaps compared to Ase1-GFP on single microtubules (Figure S3C). This computational model yielded time traces of the overlap expansion that are in good agreement with those measured experimentally (Figures 3B–3D and Movies S1 and S3). Interestingly, our computational model predicted that the total friction between two microtubules increases exponentially, instead of linearly, with the number of Ase1 crosslinkers in the overlap (Figure 3E). This non-linearity explains why our simple analytical model overestimated the sliding velocities.

To test the predicted exponential dependence of the friction on the number of crosslinkers, we characterized the Ase1-generated friction experimentally. We again formed microtubule overlaps in a similar manner as in the previous experiments (Experimental Procedures). In the absence of Ase1-GFP in solution, we observed the transport microtubules diffusing along the template microtubules (Figure S3D and Movie S4). For each transport microtubule that fully overlapped with a template microtubule, we estimated the diffusion coefficient by determining the mean square displacement as a function of time. Using the Einstein relation, we calculated the friction between the transport and the template microtubules. While a quantitative comparison between simulations and experiments was not possible due to experimental uncertainties in determining the number of crosslinkers (Experimental Procedures), the experiments confirmed the predicted exponential increase of the friction with the number of Ase1-GFP molecules as inferred from fluorescence intensities (Figure 3F).

Ase1-GFP Condensation Slows Down the Overlap Expansion

Experiments so far were performed in the absence of Ase1 in solution. In this situation, the entropic force for overlap expansion decreased with overlap length, as the available Ase1 was diluted in the overlap (Extended Results, Text 1). However, in the presence of Ase1 in solution, the binding of new crosslinkers into filament overlaps, "crosslinker condensation", generates additional forces for filament sliding (Lan et al., 2009; Peskin et al., 1993; Zandi et al., 2003). Our analytical model predicts that, in the presence of crosslinker condensation, a constant, length-independent, driving force is obtained, analogous to gas being continuously added into an expanding gas spring such that the pressure remains constant (Extended Results, Text 1). However, binding of additional crosslinkers also increases friction. The analytical model, in which the friction increases *linearly* with the number of bound crosslinkers, predicts that condensation of new crosslinkers to the expanding overlap slightly increases the velocity of overlap expansion, as compared to the case in which overlap expansion is driven by entropy alone (Extended Results, Text 1). In contrast, the computational model, in which the friction increases *exponentially* with the number of bound crosslinkers, predicts that binding of new crosslinkers to the overlap rapidly brings overlap expansion to a standstill; while crosslinker condensation keeps the driving force for overlap expansion constant, the exponential increase of the friction prohibits sliding (Figure 4A).

To test this prediction experimentally, we added assay buffer with Ase1-GFP to partially overlapping microtubules. This resulted in Ase1-GFP condensation into the overlap. We observed that the microtubules slid slower as compared to the situation without crosslinker condensation and that, in agreement with our computational model, they stopped sliding before full overlap was reached (Figures 4B, 4C, and S4). Our computational model
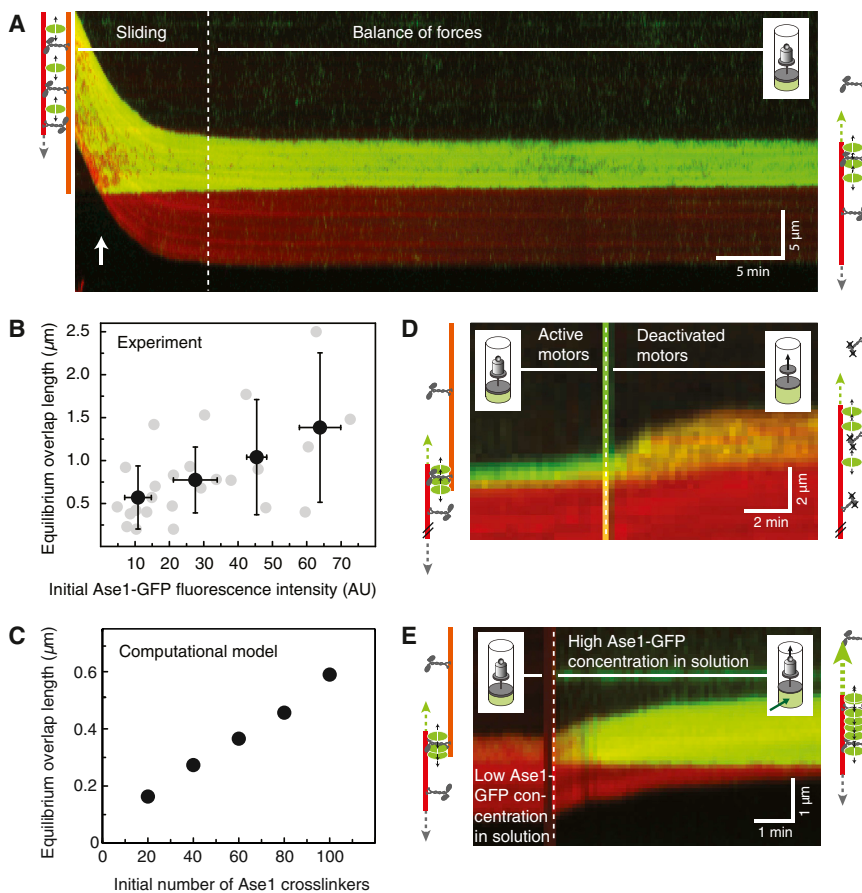
Figure 5. Ase1-Induced Entropic Forces Balance the Forces Exerted by Multiple Ncd Motors

(A) Typical multichannel kymograph showing the sliding of a transport microtubule (red) on top of an immobilized template microtubule. Partial microtubule-overlaps were formed in the presence of 312 pM Ase1-GFP (green) and 300 pM Ncd, resulting in a force equilibrium between the Ncd-motor generated force (acting in the direction of decreasing overlap length) and the Ase1-GFP entropic force (acting in the direction of increasing overlap length). The region with enhanced localization of Ase1-GFP signal corresponds to the microtubule overlap. See also Movie S5, left.

(B) At a constant Ncd concentration, the equilibrium overlap length increased with increasing amounts of Ase1-GFP in the overlap (Pearson's correlation coefficient = 0.6, p = 0.004). The length of microtubule overlaps was measured in events as presented in Figures 5A and S5B, at the moment when sliding had stopped (n = 25 events). Ase1-GFP fluorescence intensity was integrated along the overlap region at the moment when microtubules started to separate (denoted by vertical white arrow in the kymograph in A). Solid black circles represent the binned averages (±SD) of the experimental data. Data points were binned in four equidistant bins with a width of 20 AU.

(C) Results of the computational model showing the positive correlation between the initial number of crosslinkers (when the microtubules start to separate) and the equilibrium overlap length. The lengths of microtubule overlaps were determined in events as presented in Figure S5C, at the moment when sliding had effectively stopped. The motor force was modeled as an external load on the transport microtubule that scales linearly with the overlap length. The simulation parameters are summarized in Table S1.

(D) Typical multichannel kymograph (out of a total of six recorded events) demonstrating the shift of the force balance after deactivation of the Ncd-motors by exchanging ATP with ADP in the assay buffer. Driven by the entropic expansion of the Ase1-GFP molecules bound to the overlaps, the transport microtubule did slide in the direction of increasing overlap length. During the expansion phase, the Ncd-motor concentration was kept constant in solution (300 pM) and no free Ase1-GFP was present in solution. The region with enhanced localization of Ase1-GFP signal corresponds to the microtubule overlap. See also Movie S5, middle.

(E) Typical multichannel kymograph (out of a total of eight recorded events) demonstrating the shift of the force balance after increasing the Ase1-GFP concentration in solution (from 91 pM to 1,400 pM) leading to an increase in the number of Ase1-GFP molecules binding into the overlap. The transport microtubule slid in the direction of increasing overlap length; i.e., against the ATP-driven force of Ncd (kept at constant concentration of 300 pM in solution). The region with enhanced localization of Ase1-GFP signal corresponds to the microtubule overlap. See also Movie S5, right.

thus explains overlap expansion in absence (Figures 3B–3D) and presence of crosslinker condensation (Figure 4).

Ase1-Induced Entropic Forces Balance the Forces Exerted by Multiple Microtubule-Crosslinking Motors

To test whether the forces associated with the entropic expansion of the Ase1-GFP molecules are sufficient to counteract forces generated by microtubule-crosslinking motor proteins, we formed and imaged microtubule overlaps in the presence of Ase1-GFP and *D. melanogaster* kinesin-14 Ncd (Figure 5; Experimental Procedures). Ncd, which does not directly interact with Ase1 (Braun et al., 2011; Figure S5A) started to slide the microtubules apart, thereby compressing the Ase1 molecules in the shortening microtubule overlaps. During this compression, the number of bound Ase1-GFP linkers stayed roughly constant because of their high affinity for the overlap, while the number of Ncd molecules decreased linearly with decreasing overlap length (Braun et al., 2011). After about 10 min, sliding came to a halt and the lengths of the overlaps stayed constant (Figures 5A and S5B and Movie S5, left). This suggests that the sliding force induced by the Ncd motors is balanced by the entropic expansion force of Ase1, analogous to a gas spring, in which the external load is balanced by the internal pressure of the gas. The equilibrium overlap lengths increased with increasing numbers of Ase1-GFP molecules in the overlap (Figure 5B). When simulating the motor force as an external load that scales linearly with overlap length (Braun et al., 2011; Furuta et al., 2013), our computational model qualitatively reproduced both the establishment of an equilibrium state in which the overlap length becomes constant (Figure S5C) and the correlation between the number of crosslinkers in the overlap and the length of the overlap (Figure 5C; Model parameters summarized in Table S1). A quantitative comparison between experiment and simulation was not possible due to the experimental uncertainty in the number of crosslinkers

(Experimental Procedures) and the lack of information about the magnitude and scaling of the forces generated by multiple motors (Furuta et al., 2013; Nelson et al., 2014).

In line with the hypothesis that the Ncd sliding forces are balanced by the Ase1 generated forces, we found that the overlap lengths immediately increased when either (1) Ncd motors were deactivated by exchanging ATP for ADP in the assay buffer (Figure 5D and Movie S5, middle) or (2) crosslinkers were added into the overlaps by increasing the Ase1-GFP concentration in solution (Figure 5E and Movie S5, right). Hence, just like a gas spring, the overlap expanded when the force balance was tipped by either (1) reducing the opposing, external load or (2) raising the internal pressure by increasing the number of molecules in the overlap. These findings demonstrate that diffusible crosslinkers are capable of generating entropic expansion forces of the same order of magnitude as the forces generated by multiple molecular motors.

DISCUSSION

Diffusible Microtubule Crosslinkers Can Generate Entropic Forces in the pN Range
Previously, cytoskeletal re-organization has been attributed to forces either generated by molecular motors (e.g., motor-driven filament sliding in muscles, mitotic spindles, or flagella) or filament dynamics (e.g., polymerization-dependent protrusions in cell motility or depolymerization-dependent chromosome segregation). In our work, we described an additional force-generating mechanism, which is based on the entropy of diffusible crosslinkers confined between partially overlapping cytoskeletal filaments. So far, the diffusion of proteins along cytoskeletal filaments has been mostly associated with the generation of mechanical friction in response to sliding movement (Bormuth et al., 2009; Braun et al., 2011; Forth et al., 2014; Janson et al., 2007; Subramanian et al., 2010). However, diffusion inside a confined space also creates a pressure that can manifest itself as a directed entropic force even in the absence of other forces. Notably, this mechanism is different from mechanisms based on condensation, which have previously been put forward as alternative force-generating mechanisms in a number of different contexts including thermal ratchets (Gayathri et al., 2012; Hill, 1985; Lan et al., 2009; Neujahr et al., 1997; Peskin et al., 1993; Sun et al., 2010; Zandi et al., 2003). Employing the diffusible microtubule crosslinker Ase1, we demonstrated the entropic force generation against three different external forces, i.e., originating from hydrodynamic flow, optical tweezers, and molecular motors. In line with the prediction of our analytical model, optical tweezers measurements revealed that the entropic forces were in the pN range when the binding sites within the overlaps were highly occupied by the Ase1-GFP molecules (Figure 2C; Extended Results). In agreement with an entropic driving force, we observed a linear increase of force with crosslinker density (Figures 2C, inset, and S2C).

Entropic Forces Are High Enough to Balance the Forces of Motor Proteins
The crosslinker-induced forces observed in our experiments and described by our models are comparable to the forces gener-

ated by multiple molecular motors (Figure 5). Molecular motors that regulate the length of the midzone of the mitotic spindle slide overlapping microtubules apart, thereby decreasing the lengths of the microtubule overlaps (Fink et al., 2009; Kapitein et al., 2005). Our work suggests that this motion will compact the crosslinkers that are localized in the midzone overlaps (Schuyler et al., 2003; Yamashita et al., 2005), generating entropic forces that oppose the motor-driven sliding. For kinesin-14 Ncd, which is capable of exerting additive forces of about 0.1 pN per motor (Furuta et al., 2013), we were able to directly show the balance between motor forces and entropic forces. For stronger motors involved in spindle organization, such as kinesin-5, which generates forces of 5–7 pN per motor (Valentine et al., 2006), the entropic forces may not be able to fully antagonize the motor forces. However, forces generated by multiple molecular motors do not necessarily add up (Furuta et al., 2013). Moreover, recent work on Cin8 (yeast kinesin-5) shows that motors can switch directionality (Roostalu et al., 2011). Thus, the force generated by multiple kinesin-5 motors might be much lower than the simple sum of the maximal forces that are generated by each individual motor. In such cases, and in situations where motors of different types compete with one another (Hentrich and Surrey, 2010), Ase1 could play a major role in setting the force balance. Ase1-induced entropic forces may indeed help to stabilize overlaps in the spindle midzones during mitosis, where ensembles of molecular motors are involved in the control of microtubule sliding.

Our results suggest that entropic expansion and condensation of Ase1, as well as of other diffusible microtubule crosslinkers, constitute an additional layer of regulation for the dynamic control of microtubule overlap length, besides the regulation of microtubule dynamics (Bieling et al., 2010) and force production by opposing molecular motors (Hentrich and Surrey, 2010). Phospho-regulation of Ase1 during the cell cycle (Fu et al., 2009) could regulate the difference in affinity of crosslinkers for microtubule overlaps and for single microtubules. This would enable control over the magnitudes of the entropic and condensation forces.

In the future, it will be interesting to study entropic force generation with proteins from other organisms. Although the vertebrate Ase1 homolog PRC1 unbinds faster from microtubules then Ase1, similarly to Ase1, PRC1 has a preference for binding to microtubule overlaps compared to binding to single microtubules (Bieling et al., 2010). PRC1 is thus also confined between overlapping microtubules, and since it is diffusible, is likely to generate entropic forces. Extensive in vivo work will be necessary to determine the magnitude of the crosslinker-induced forces in the different scenarios. Besides the generation of forces between anti-parallel microtubules, diffusible crosslinkers may also exert forces between parallel microtubules. In such a geometry, where crosslinking motors fail to generate directed motion (Braun et al., 2009; Fink et al., 2009; Kapitein et al., 2005), overlap maximization may aid the focusing of parallel microtubules into poles in the absence of centrosomes (Compton, 1998).

Crosslinker Friction Scales Exponentially with Crosslinking Number
When new crosslinkers condense into the expanding overlap, the friction between the microtubules rises. Our computational

model predicts that the friction scales exponentially—rather than linearly—with the number of crosslinking Ase1 molecules (Figure 3E). Our experiments provide three independent lines of evidence for this non-linear behavior: (1) the sliding velocities measured in the absence of crosslinker condensation (Figures 3B–3D), as well as (2) the halting of overlap expansion in the presence of crosslinker condensation (Figure 4) cannot be explained by a linear model, and (3) direct measurements of the friction coefficient as a function of the number of crosslinking Ase1 molecules show an exponential relation (Figure 3F). Ase1 oligomerization (as reported in Kapitein et al., 2008) could potentially result in superlinear scaling, because the movement of the monomers in an oligomer becomes tightly coupled. However, under our experimental conditions we did not observe Ase1 oligomers (e.g., Figures 1D, 4B, 5D, and 5E). Moreover, the Hill coefficient for Ase1 binding was very low (Figure S3A), indicating that binding is essentially non-cooperative and that the energetic interactions between the bound Ase1 molecules were very weak. In our computational model, we therefore assumed that Ase1 binds non-cooperatively to microtubules, and we nonetheless found that the friction increases exponentially with the number of crosslinkers (Figure 3E). We attribute the exponential scaling of the friction to the fact that filament movement is a collective and activated process that requires the "simultaneous" hopping (i.e., transient unbinding) of multiple crosslinkers. This process involves the crossing of an energy barrier that increases linearly with the number of crosslinkers, leading to an exponential decrease in the rate of crossing the barrier (Erickson, 2009; Volkov et al., 2013) (Extended Results, Text 4). We hypothesize that this mechanism might be relevant also for other processes where cellular structures are tethered to microtubules. For example, fewer microtubule-interacting proteins than expected based on a linear dependence of the friction may be sufficient to forcefully tether kinetochores to microtubules.

Entropic Forces Are Generated whenever Molecular Diffusion Is Confined

The mechanism of entropic force generation by confined molecules is a universal phenomenon beyond the Ase1/PRC1/MAP65 family of microtubule crosslinking proteins. Recently, nucleosome unwrapping was quantitatively explained by the one-dimensional pressure exerted by DNA binding proteins diffusing along a DNA strand (Forties et al., 2011). Furthermore, entropic forces are also generated in 2D systems, which is exemplified by the finding that crowding of membrane-bound proteins generates a lateral pressure, which can bend membranes (Stachowiak et al., 2012). Concerning the cytoskeleton, it has long been believed that the constriction of the actin contractile ring is driven by non-muscle myosin II (NMII) translocation of actin filaments. However, recent experiments indicate that NMII is required not for its motor activity to translocate actin, but for its capacity to crosslink actin filaments (Ma et al., 2012). Our results suggest that NMII may be able to generate tension between actin filaments via the mechanism of entropic expansion if it can diffuse between filaments.

Our in vitro system allows for the well-controlled experimental investigation of the interplay between entropic-expansion forces, crosslinker-condensation forces, and crosslinker-frictional forces that drive the sliding of filaments relative to each other. By examining a minimal system consisting of crosslinkers and microtubules, outside of the cytoplasm, we gain access to biophysical properties of the system that are impossible to access in vivo where they are obscured by numerous interdependent processes. Taken together, our results demonstrate that the thermal motion of confined crosslinkers constitutes a force-producing element within self-organizing filamentous networks, which can complement forces generated by molecular motors and filament dynamics.

EXPERIMENTAL PROCEDURES

Protein Purification

Recombinant histidine-tagged full-length *S. pombe* Ase1-GFP (Figure S1A) and *D. melanogaster* Ncd and GFP-Ncd were expressed and purified as described previously (Fink et al., 2009; Janson et al., 2007).

Sample Preparation

Microtubules and flow chambers were prepared as described previously (Fink et al., 2009). If not noted otherwise, dimly rhodamine-labeled, biotinylated template microtubules in BRB80 buffer (80 millimolar (mM) PIPES, 1 mM EGTA, 1 mM $MgCl_2$, 10 μM paclitaxel, pH 6.9) were injected into the flow chamber and bound in an aligned manner to surface-immobilized biotin anti-bodies (Sigma, B3640). After rinsing the chamber with assay buffer (20 mM HEPES at pH 7.2, 1 mM EGTA, 0.1 mM EDTA, 75 mM KCl, 1 mM ATP (+Mg), 10 mM DTT, 0.5 mg/ml casein, 10 μM paclitaxel, 0.1% Tween, 20 mM D-glucose, 110 μg/ml glucose oxidase, and 20 μg/ml catalase), 50 pM Ase1-GFP was flushed in, which bound to the template microtubules. In the next step, brightly rhodamine-labeled transport microtubules were flushed in (without Ase1-GFP in that solution) and allowed to bind to the template microtubules that were still covered sparsely with Ase1-GFP. For hydrodynamic flow experiments, finally a 30 s long steady flow of assay buffer (without Ase1-GFP) was applied to shorten the microtubule overlaps by sliding the transport microtubules along the template microtubules, while concurrently removing all unbound transport microtubules. For Ase1-condensation experiments the duration of the final step was 5 s and the buffer included 17 pM Ase1-GFP. For Ncd-Ase1-sliding experiments, the duration of the final step was 5 s and the buffer included 312 pM Ase1-GFP and 300 pM Ncd. For microtubule-microtubule diffusion experiments the template microtubules were Cy-5 labeled in order to allow for high-precision position tracking of the brightly rhodamine-labeled transport microtubules (since tracking accuracy would be impaired if transport and template microtubules had the same fluorescent label) and the duration of the final step was approximately 5 s. For optical trapping experiments dimly Cy5-labeled, digoxigeninated template microtubules in BRB80 buffer were bound to surface-immobilized digoxigenin anti-bodies (Roche, # 11333089001). After rinsing the chamber with assay buffer, Ase1-GFP was flushed in and brightly Cy5-labeled, biotinylated transport microtubules were subsequently flushed in (no Ase1-GFP in solution, neither here, nor in the following steps). In the next step, assay buffer with NeutrAvidin coated silica microspheres was applied. Using a trapped microsphere attached to a biotinylated transport microtubule, overlaps were shortened by moving the template microtubule with a piezo stage.

Image Acquisition during Hydrodynamic Flow, Microtubule-Microtubule Diffusion, Ase1-Condensation, and Ncd-Ase1-Sliding Experiments

Rhodamine-labeled microtubules, Cy-5 labeled microtubules, and Ase1-GFP were visualized sequentially by switching between tetramethylrhodamine isothiocyanate (TRITC), Cy-5, and GFP filters (Chroma Technology), respectively, using a previously described setup (Fink et al., 2009) with acquisition rates of one frame per 6 or 30 s (time-lapse information indicated in the figures).

Image Analysis of Microtubule-Microtubule Sliding and Diffusion Experiments

In the hydrodynamic flow, Ase1-condensation and Ncd-sliding experiments the positions of the transport microtubules relative to the template microtubules were determined in each frame. Partial microtubule-overlaps had a non-moving boundary (corresponding to the end of the template microtubule, which is fixed on the coverslip) and a moving boundary (corresponding to the end of the transport microtubule, which moves along the template). The moving ends were read out from the TRITC channel as the positions of the transport microtubule ends. Using the fact that Ase1-GFP bound more strongly to the overlaps as compared to single microtubules, the non-moving ends were read out from the GFP channel as the positions of the edges of the GFP signals averaged over all frames of a time-lapse movie. Sliding velocities were obtained from positional data of the transport microtubules using a rolling frame average over five frames. In the microtubule-microtubule diffusion experiments, image analysis was performed similarly to the experiments described above with the exception of using a high-precision tracking software, Fiesta, to determine the drift corrected positions of the transport microtubules (Ruhnow et al., 2011). Drift correction was performed in Fiesta by tracking the positions of 200 nanometer (nm) TetraSpeck beads (Life Technologies) non-specifically attached to the coverslip surface.

Optical Trapping and Analysis

An optical tweezers setup (JPK Instruments, NanoTracker) was built on a Nikon eclipse T*i* microscope equipped with a Nikon TIRF 60× N.A. 1.49 objective. Lateral bead positions were inferred by back focal plane detection using a quadrant photo diode. Sensitivity and stiffness were obtained using a built-in calibration feature that fits a Lorentzian function to the power spectrum of the thermal fluctuations of a trapped bead. Carboxylated silica beads (Bangs Laboratories, #SC04N) were functionalized with NeutrAvidin (ThermoScientific) using 1-Ethyl-3-(3-dimethylaminopropyl)carbodiimide-N-hydroxysulfosuccinimide chemistry. All measurements were performed at a trap stiffness of approximately 0.15 pN/nm (750 milliwatt optical power of a 1,064 nm infrared-laser), and the time traces were recorded with 5 kHz sampling rate. The time traces were converted from voltages to forces and further analyzed using MATLAB. A constant offset, given by the averaged signal after microtubule separation, was subtracted from all forces. To estimate the Ase1-generated entropic forces, we averaged the detected forces starting after 2 s relaxation time after each rapid movement of the piezo stage (see Figure S2B). In Figure 2C, we only present data that were recorded after the bead was pulled past the end of the template microtubule, such that the forces applied to the overlap were solely pulling forces. Negative forces with amplitudes smaller than 0.5 pN were occasionally observed in individual traces due to drift in the optical tweezers setup. For optical imaging, the tweezers setup was equipped with a Nikon TIRF microscopy unit, which was used to visualize the microtubule overlaps. Cy5-labeled microtubules and Ase1-GFP were excited sequentially using 642 nm and 488 nm lasers (Vortran) and a dual-band filter set (Chroma Technology). Image acquisition was performed by a back illuminated EMCCD camera (Andor) at rates of one frame per 10 s (time-lapse information indicated in the figures) using Micro-Manager software (Edelstein et al., 2010).

Estimating the Number of GFP-Ase1 Molecules in Microtubule Overlaps

The location of a microtubule overlap (either determined by the enhanced GFP-signal or the positions of the template and transport microtubules) was used as mask to read out the integrated Ase1-GFP signal in an overlap. The fluorescence signal (obtained with the same filter set) integrated over the same mask area directly adjacent to the overlap was subtracted as the background signal. The "Ase1-GFP fluorescence intensity" in a microtubule overlap (as used in Figures 2C inset, 3F, 4C, and 5B) was then calculated by dividing the background-corrected integrated Ase1-GFP signal by the fluorescence signal of a single Ase1-GFP molecule, as described previously (Braun et al., 2011). The Ase1-GFP fluorescence intensity thus provides a rough estimate of the absolute number of GFP-Ase1 molecules in a microtubule overlap and can, most importantly, be used to study entropic force, friction, and overlap length as function of relative changes in the number of GFP-Ase1 molecules in an overlap. However, due to significant errors inherently associated

with the described procedure (e.g., experimental uncertainties due to GFP bleaching and blinking, as well as the uneven TIRF illumination, the extent of which may vary from experiment to experiment), we refrain from equating the Ase1-GFP fluorescence intensity with the actual number of GFP-Ase1 molecules in a microtubule overlap and rather express it in AU.

REFERENCES

Asbury, C.L., Gestaut, D.R., Powers, A.F., Franck, A.D., and Davis, T.N. (2006). The Dam1 kinetochore complex harnesses microtubule dynamics to produce force and movement. Proc. Natl. Acad. Sci. USA *103*, 9873–9878.

Bieling, P., Telley, I.A., and Surrey, T. (2010). A minimal midzone protein module controls formation and length of antiparallel microtubule overlaps. Cell *142*, 420–432.

Bormuth, V., Varga, V., Howard, J., and Schäffer, E. (2009). Protein friction limits diffusive and directed movements of kinesin motors on microtubules. Science *325*, 870–873.

Braun, M., Drummond, D.R., Cross, R.A., and McAinsh, A.D. (2009). The kinesin-14 Klp2 organizes microtubules into parallel bundles by an ATP-dependent sorting mechanism. Nat. Cell Biol. *11*, 724–730.

Braun, M., Lansky, Z., Fink, G., Ruhnow, F., Diez, S., and Janson, M.E. (2011). Adaptive braking by Ase1 prevents overlapping microtubules from sliding completely apart. Nat. Cell Biol. *13*, 1259–1264.

Civelekoglu-Scholey, G., and Scholey, J.M. (2010). Mitotic force generators and chromosome segregation. Cell. Mol. Life Sci. *67*, 2231–2250.

Compton, D.A. (1998). Focusing on spindle poles. J. Cell Sci. *111*, 1477–1481.

Edelstein, A., Amodaj, N., Hoover, K., Vale, R., and Stuurman, N. (2010). Computer control of microscopes using µManager. Curr. Protoc. Mol. Biol. *Chapter 14*, Unit14.20.

Einstein, A. (1906). Zur theorie der Brownschen bewegung. Annalen der Physik *19*, 371–381.

Erickson, H.P. (2009). Modeling the physics of FtsZ assembly and force generation. Proc. Natl. Acad. Sci. USA *106*, 9238–9243.

Fink, G., Hajdo, L., Skowronek, K.J., Reuther, C., Kasprzak, A.A., and Diez, S. (2009). The mitotic kinesin-14 Ncd drives directional microtubule-microtubule sliding. Nat. Cell Biol. *11*, 717–723.

Forth, S., Hsia, K.-C., Shimamoto, Y., and Kapoor, T.M. (2014). Asymmetric friction of nonmotor MAPs can lead to their directional motion in active microtubule networks. Cell *157*, 420–432.

Forties, R.A., North, J.A., Javaid, S., Tabbaa, O.P., Fishel, R., Poirier, M.G., and Bundschuh, R. (2011). A quantitative model of nucleosome dynamics. Nucleic Acids Res. *39*, 8306–8313.

Fu, C., Ward, J.J., Loïodice, I., Velve-Casquillas, G., Nedelec, F.J., and Tran, P.T. (2009). Phospho-regulated interaction between kinesin-6 Klp9p and microtubule bundler Ase1p promotes spindle elongation. Dev. Cell *17*, 257–267.

Furuta, K., Furuta, A., Toyoshima, Y.Y., Amino, M., Oiwa, K., and Kojima, H. (2013). Measuring collective transport by defined numbers of processive and nonprocessive kinesin motors. Proc. Natl. Acad. Sci. USA *110*, 501–506.

Gayathri, P., Fujii, T., Møller-Jensen, J., van den Ent, F., Namba, K., and Löwe, J. (2012). A bipolar spindle of antiparallel ParM filaments drives bacterial plasmid segregation. Science *338*, 1334–1337.

Gestaut, D.R., Graczyk, B., Cooper, J., Widlund, P.O., Zelter, A., Wordeman, L., Asbury, C.L., and Davis, T.N. (2008). Phosphoregulation and depolymerization-driven movement of the Dam1 complex do not require ring formation. Nat. Cell Biol. *10*, 407–414.

Helenius, J., Brouhard, G., Kalaidzidis, Y., Diez, S., and Howard, J. (2006). The depolymerizing kinesin MCAK uses lattice diffusion to rapidly target microtubule ends. Nature *441*, 115–119.

Hentrich, C., and Surrey, T. (2010). Microtubule organization by the antagonistic mitotic motors kinesin-5 and kinesin-14. J. Cell Biol. *189*, 465–480.

Hill, T.L. (1985). Theoretical problems related to the attachment of microtubules to kinetochores. Proc. Natl. Acad. Sci. USA *82*, 4404–4408.

Hunt, A.J., Gittes, F., and Howard, J. (1994). The force exerted by a single kinesin molecule against a viscous load. Biophys. J. *67*, 766–781.

Janson, M.E., Loughlin, R., Loïodice, I., Fu, C., Brunner, D., Nédélec, F.J., and Tran, P.T. (2007). Crosslinkers and motors organize dynamic microtubules to form stable bipolar arrays in fission yeast. Cell *128*, 357–368.

Kapitein, L.C., Peterman, E.J.G., Kwok, B.H., Kim, J.H., Kapoor, T.M., and Schmidt, C.F. (2005). The bipolar mitotic kinesin Eg5 moves on both microtubules that it crosslinks. Nature *435*, 114–118.

Kapitein, L.C., Janson, M.E., van den Wildenberg, S.M.J.L., Hoogenraad, C.C., Schmidt, C.F., and Peterman, E.J.G. (2008). Microtubule-driven multimerization recruits ase1p onto overlapping microtubules. Curr. Biol. *18*, 1713–1717.

Lan, G., Daniels, B.R., Dobrowsky, T.M., Wirtz, D., and Sun, S.X. (2009). Condensation of FtsZ filaments can drive bacterial cell division. Proc. Natl. Acad. Sci. USA *106*, 121–126.

Loïodice, I., Staub, J., Setty, T.G., Nguyen, N.P., Paoletti, A., and Tran, P.T. (2005). Ase1p organizes antiparallel microtubule arrays during interphase and mitosis in fission yeast. Mol. Biol. Cell *16*, 1756–1768.

Ma, X., Kovács, M., Conti, M.A., Wang, A., Zhang, Y., Sellers, J.R., and Adelstein, R.S. (2012). Nonmuscle myosin II exerts tension but does not translocate actin in vertebrate cytokinesis. Proc. Natl. Acad. Sci. USA *109*, 4509–4514.

Nelson, S.R., Trybus, K.M., and Warshaw, D.M. (2014). Motor coupling through lipid membranes enhances transport velocities for ensembles of myosin Va. Proc. Natl. Acad. Sci. USA *111*, E3986–E3995.

Neujahr, R., Heizer, C., and Gerisch, G. (1997). Myosin II-independent processes in mitotic cells of Dictyostelium discoideum: redistribution of the nuclei, re-arrangement of the actin system and formation of the cleavage furrow. J. Cell Sci. *110*, 123–137.

Peskin, C.S., Odell, G.M., and Oster, G.F. (1993). Cellular motions and thermal fluctuations: the Brownian ratchet. Biophys. J. *65*, 316–324.

Peterman, E.J.G., and Scholey, J.M. (2009). Mitotic microtubule crosslinkers: insights from mechanistic studies. Curr. Biol. *19*, R1089–R1094.

Powers, A.F., Franck, A.D., Gestaut, D.R., Cooper, J., Gracyzk, B., Wei, R.R., Wordeman, L., Davis, T.N., and Asbury, C.L. (2009). The Ndc80 kinetochore complex forms load-bearing attachments to dynamic microtubule tips via biased diffusion. Cell *136*, 865–875.

Roostalu, J., Hentrich, C., Bieling, P., Telley, I.A., Schiebel, E., and Surrey, T. (2011). Directional switching of the kinesin Cin8 through motor coupling. Science *332*, 94–99.

Ruhnow, F., Zwicker, D., and Diez, S. (2011). Tracking single particles and elongated filaments with nanometer precision. Biophys. J. *100*, 2820–2828.

Schuyler, S.C., Liu, J.Y., and Pellman, D. (2003). The molecular function of Ase1p: evidence for a MAP-dependent midzone-specific spindle matrix. Microtubule-associated proteins. J. Cell Biol. *160*, 517–528.

Stachowiak, J.C., Schmid, E.M., Ryan, C.J., Ann, H.S., Sasaki, D.Y., Sherman, M.B., Geissler, P.L., Fletcher, D.A., and Hayden, C.C. (2012). Membrane bending by protein-protein crowding. Nat. Cell Biol. *14*, 944–949.

Subramanian, R., Wilson-Kubalek, E.M., Arthur, C.P., Bick, M.J., Campbell, E.A., Darst, S.A., Milligan, R.A., and Kapoor, T.M. (2010). Insights into antiparallel microtubule crosslinking by PRC1, a conserved nonmotor microtubule binding protein. Cell *142*, 433–443.

Sun, S.X., Walcott, S., and Wolgemuth, C.W. (2010). Cytoskeletal cross-linking and bundling in motor-independent contraction. Curr. Biol. *20*, R649–R654.

Tawada, K., and Sekimoto, K. (1991). Protein friction exerted by motor enzymes through a weak-binding interaction. J. Theor. Biol. *150*, 193–200.

Valentine, M.T., Fordyce, P.M., Krzysiak, T.C., Gilbert, S.P., and Block, S.M. (2006). Individual dimers of the mitotic kinesin motor Eg5 step processively and support substantial loads in vitro. Nat. Cell Biol. *8*, 470–476.

Volkov, V.A., Zaytsev, A.V., Gudimchuk, N., Grissom, P.M., Gintsburg, A.L., Ataullakhanov, F.I., McIntosh, J.R., and Grishchuk, E.L. (2013). Long tethers provide high-force coupling of the Dam1 ring to shortening microtubules. Proc. Natl. Acad. Sci. USA *110*, 7708–7713.

Yamashita, A., Sato, M., Fujita, A., Yamamoto, M., and Toda, T. (2005). The roles of fission yeast ase1 in mitotic cell division, meiotic nuclear oscillation, and cytokinesis checkpoint signaling. Mol. Biol. Cell *16*, 1378–1395.

Zandi, R., Reguera, D., Rudnick, J., and Gelbart, W.M. (2003). What drives the translocation of stiff chains? Proc. Natl. Acad. Sci. USA *100*, 8649–8653.